Neuron, Vol. 20, 1111–1122, June, 1998, Copyright ©1998 by Cell Press

Subunit Composition, Protein Interactions, and Structures of the Mammalian Brain sec6/8 Complex and Septin Filaments

Shu-Chan Hsu,* Christopher D. Hazuka,*
Robyn Roth,† Davide L. Foletti,*
John Heuser,† and Richard H. Scheller*‡
*Howard Hughes Medical Institute
Department of Molecular and Cellular Physiology
Stanford University School of Medicine
Stanford, California 94305
†Department of Cell Biology and Physiology
Washington University School of Medicine
St. Louis, Missouri 63110

Summary

Both the sec6/8 complex and septin filaments have been implicated in directing vesicles and proteins to sites of active membrane addition in yeast. The rat brain sec6/8 complex coimmunoprecipitates with a filament composed of four mammalian septins, suggesting an interaction between these complexes. One of the septins, CDC10, displays broad subcellular and tissue distributions and is found in postmitotic neurons as well as dividing cells. Electron microscopic studies showed that the purified rat brain septins form filaments of 8.25 nm in diameter; the lengths of the filaments are multiples of 25 nm. Glutaraldehyde-fixed rat brain sec6/8 complex adopts a conformation resembling the letter "T" or "Y". The sec6/8 and septin complexes likely play an important role in trafficking vesicles and organizing proteins at the plasma membrane of neurons.

Introduction

The sorting and targeting of secretory vesicles to specific docking and fusion sites is essential for the appropriate organization of membrane compartments in the cell. Following their biogenesis, Golgi-derived secretory vesicles are likely to be guided toward the plasma membrane by specific motors moving along cytoskeletal networks. Once they are in the vicinity of their target sites, one or more recognition events mediates the docking of these vesicles to the plasma membrane. After this initial recognition event, additional biochemical reactions activate the fusion apparatus eventually resulting in the merger of the vesicle membrane with the plasma membrane, either in a regulated or in a constitutive manner. Since fidelity of the vesicle targeting and trafficking process is essential for cell growth, differentiation, and survival, the molecular mechanisms underlying this pathway have been intensely investigated.

Genetic, cell biological, and biochemical studies in yeast and mammals have identified and characterized many proteins involved in the secretory vesicle trafficking process (Scheller, 1995; Südhof, 1995; Rothman and Wieland, 1996). Interactions between these proteins are thought to comprise the biochemical pathway leading to vesicle docking and membrane fusion. A key "core complex" is formed between the synaptic vesicle protein, VAMP/synaptobrevin, and two plasma membrane proteins, syntaxin and SNAP-25. Formation of this heterotrimeric complex has been implicated in juxtaposing the synaptic vesicle and the plasma membrane, leading to membrane fusion (Lin and Scheller, 1997; Hanson et al., 1997). Both syntaxin and VAMP are members of protein families and individual members of these two protein families have distinct tissue and subcellular distributions (Hay and Scheller, 1997). The combinatorial interactions among members of these protein families has been proposed to play a role in determining vesicle targeting fidelity. However, synaptic vesicles still appear morphologically docked at active zones in *Drosophila* mutants missing syntaxin and in synapses following the cleavage of VAMP, syntaxin, or SNAP-25 by botulinum and tetanus toxins. These results suggest that the interactions among these three proteins mediate a postdocking event (Hunt et al., 1994; Broadie et al., 1995). Additionally, immunohistochemical studies showed that both syntaxin and SNAP-25, as well as their homologs in yeast, have a diffuse localization on the plasma membrane that does not reflect topographic variations in the levels of secretory events, which often occur at specialized domains (Catsicas et al., 1992; Oyler et al., 1992; Koh et al., 1993; Garcia et al., 1995). Thus, while the trimeric VAMP/syntaxin/SNAP-25 complex plays a critical role in ensuring specificity of the eventual fusion of the secretory vesicle with its correct target membrane, this complex is not likely to be involved in the initial events that mediate the targeting and docking of secretory vesicles.

A potential candidate for these initial targeting and docking reactions is the sec6/8 (or exocyst) complex. This complex is required for exocytosis; mutations in any of the seven genes whose products comprise the yeast sec6/8 complex result in an accumulation of secretory vesicles within the bud of the yeast daughter cell (Novick et al., 1980; TerBush et al., 1996). The conservation of the sec6/8 complex in mammalian species, its ubiquitous expression in multiple tissues, and the early embryonic lethality of mice containing a mutation in one of its subunits (sec8) suggest that it may be a widely utilized component of the exocytic machinery (Ting et al., 1995; Hsu et al., 1996; Friedrich et al., 1997). Several observations suggest that the sec6/8 complex may function in the targeting and docking of secretory vesicles to appropriate sites on the plasma membrane. First, the yeast sec6/8 complex is recruited to sites of membrane addition during the budding process (Mondésert et al., 1997). At an early stage of the yeast budding process, the sec6/8 complex is recruited to the tip of the developing daughter cell, where polarized membrane addition takes place to support daughter cell growth. Later, during cytokinesis, the yeast complex is found concentrated at the mother–daughter cell boundary, where membrane expansion is required to complete the separation of the daughter cell from the mother cell.

‡To whom correspondence should be addressed.

Second, the yeast sec6/8 complex has been implicated in organizing the bud site in yeast. Mutations in sec3 and sec5, two subunits of the yeast complex, result in random bud site selection (Finger and Novick, 1997; Mondésert et al., 1997). The sec6/8 complex may either directly target vesicles to appropriate sites to initiate budding or, alternatively, recruit other proteins to the plasma membrane to set up a "targeting patch," which then directs vesicles to the predetermined budding sites. Third, yeast genetic studies showed that overexpression of sso1p, a yeast homolog of the mammalian syntaxin, can suppress mutations in sec3 and sec15, two subunits of the yeast complex, suggesting that the sec6/8 complex acts upstream of membrane fusion events (Aalto et al., 1993). Finally, the introduction of monoclonal antibodies against rat sec8, a subunit of the rat sec6/8 complex, into permeabilized MDCK cells inhibited vesicle transport to the basolateral plasma membrane domain of these cells (K. Grindstaff, C. Yeaman, N. Anandasabapathy, S.-C. H., E. Rodriguez-Boulan, R. H. S., and W. J. Nelson, submitted). These results suggest that the sec6/8 complex functions in vesicle targeting and docking events upstream of the fusion events mediated by the VAMP/syntaxin/SNAP-25 trimeric complex in yeast and mammals.

To investigate the function of the sec6/8 complex in vesicle trafficking, we isolated and characterized interacting proteins. In this paper, we describe the in vitro association of the sec6/8 complex with a filament comprised of septins. The septins are a family of GTPases, conserved across species, which form plasma membrane-associated filaments. While the septins have been most intensely studied for their role in cytokinesis (reviewed by Sanders and Field, 1994; Longtine et al., 1996), our data suggest a general role in plasma membrane protein organization in neurons. We have also visualized the purified rat brain sec6/8 and septin complexes by quick-freeze, deep-etch electron microscopy. The sec6/8 complex and the septin filaments may associate to provide a targeting system to recruit secretory vesicles to appropriate docking/fusion sites leading to the proper organization of proteins along the plasma membrane.

Results

Association of the Rat Brain sec6/8 Complex with Rat Septin Proteins

To better understand the mechanism of sec6/8 complex function in vesicle trafficking, immunoprecipitation studies were carried out to isolate and identify associated proteins. Three monoclonal antibodies, 2E12, 5C3, and 10C2, were generated against rat sec8 (Hsu et al., 1996). Western blot analysis shows that all three antibodies recognize a single protein band corresponding to rat sec8 at 110 kDa in total brain homogenate (Figure 1A). All three monoclonal antibodies immunoprecipitate the sec6/8 complex from total soluble rat brain proteins. Figure 1B shows a typical immunoprecipitation result using the 2E12 monoclonal antibody. The anti-rat sec8 monoclonal antibody, but not the nonspecific control mouse immunoglobulins, immunoprecipitated eight protein bands ranging from 70–110 kDa; these bands correspond to the subunits of the sec6/8 complex. In addition,

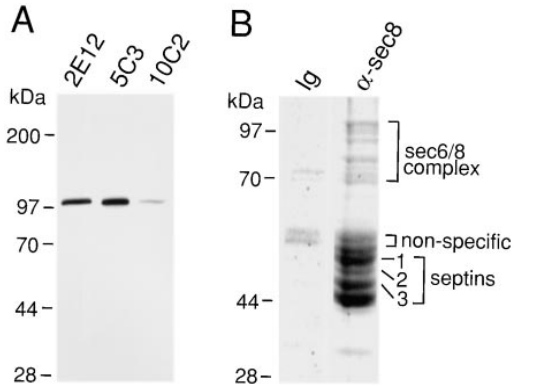

Figure 1. Septin Proteins Coimmunoprecipitate with the sec6/8 Complex

(A) Western blot analysis of anti-rat sec8 monoclonal antibodies 2E12, 5C3, and 10C2. Frozen rat brains were boiled in a protein-loading buffer containing 10% SDS before fractionation on an 8% SDS-polyacrylamide gel. Approximately 25 μg of total brain protein was loaded per lane.

(B) Coomassie Blue–stained SDS-PAGE analysis of immunoprecipitations by nonspecific control immunoglobulin (Ig) or by anti-rat sec8 monoclonal antibody 2E12 (α-sec8).

there were also six major protein bands ranging from 44–60 kDa, which coimmunoprecipitated with the sec6/8 complex. The first two protein bands are probably nonspecific since they also bind to the control mouse immunoglobulins. To identify the remaining specific protein bands, three bands (shown in Figure 1) were excised from the gel, digested with trypsin, and subjected to peptide sequencing. Comparison of the obtained peptide sequences with GenBank databases identified these proteins to be rat equivalents of human and mouse septin proteins (Table 1 and Figure 7, bands 1–3). These results suggest that the sec6/8 complex can associate with mammalian septin proteins. It is possible that these septin proteins are components of a rat septin complex analogous to the yeast neck filament composed of cdc3p, cdc10p, cdc11p, and cdc12p (reviewed by Longtine et al., 1996) and to the *Drosophila* septin complex containing PNUT, Sep2, and Sep3 (Field et al., 1996).

Distribution and Localization of Rat CDC10

To begin characterization of the rat septin proteins, polyclonal antibodies were generated against one of the septins, CDC10. The anti-CDC10 rabbit polyclonal antibodies, but not the preimmune serum, recognize two closely spaced immunoreactive bands at the expected molecular weight (50 kDa) corresponding to CDC10 in total brain homogenate (Figure 2A). CDC10 is most abundant in brain and lung, but is also expressed in smaller amounts in pancreas and testes (Figure 2B). The tissue-specific expression of CDC10 suggests that different cells may require specific isoforms of CDC10 for functions characteristic of those cell types.

The septins are best known for their strategic location at the mother–daughter cell boundary during cytokinesis (reviewed by Sanders and Field, 1994; Longtine et al., 1996). Labeling of Triton X-100–extracted dividing MDCK cells by anti-CDC10 antibodies confirmed that

Table 1. Subunits of the Rat Brain Septin Complex

Band 1 KIAA0128	
(52 kDa)	
KIAA0128 (D50918)	
LTIVSTVGFGDQI	aa 94–106
VNIIPIIAK	aa 174–182
ARQYPWQTVQVENE	aa 249–263
PFSLQETYEAK	aa 314–324
RNEFLGELK	aa 325–334
KEEEMRQMFVQR	aa 335–346
Band 2 KIAA0128/CDC10	
(50 kDa)	
KIAA0128 (D50918)	
STLMDTLFNTK	aa 53–63
LDLVTMK	aa 162–168
VNIIPIIAK	aa 174–182
hCDC10 (S72008)	
NLEGYVGFANLPNQVYRK	aa 6–24
STLINSLFLTDL	aa 45–56
RLPLAVVGSN	aa 224–233
Band 3 CDC10	
(48 kDa)	
hCDC10 (S72008)	
NLEGYVGFANLP	aa 6–18
RGFEFTLM	aa 28–35
DVTNNVHYENYR	aa 279–291
DSEAELQRRHEQ	aa 355–366
Band 4 DIFF6	
(46 kDa)	
HUMDIFF6 (D28540, D28509)	
MusNEDD5 (D49382, D10915, D26128)	
KIAA0158 (D63878)	
QQPTQFINPETPGYVG	aa 4–19
STLINSLFLTDLYPER	aa 51–66
VNIVPVIAK	aa 175–183
RILDEIEEHNIK	aa 198–209
huH5 (U59632)	
hCDCrel-1 (U74628)	
huPNUTL1 (Y11593)	
STLVHSLFLTD	aa 57–68
NIQDNRVHCCLY	aa 147–158
Band 5 H5	
(44 kDa)	
huH5 (U59632)	
hCDCrel-1 (U74628)	
huPNUTL1 (Y11593)	
QYVGFATLPNQVH	aa 23–35
STLVHSLFLTD	aa 58–68
ESAPFAVIGSNTVVEAK	aa 239–256

To identify the subunits of the septin complex, peptides derived from each of the five septin bands (Bands 1–5; Figure 7) were screened against GenBank databases. Peptides from each band are listed below their respectively matched proteins, and their positions in these proteins are shown beside each peptide sequence. The GenBank accession number of each matched protein is shown in brackets. When there are multiple GenBank entries for the same protein, all entries, with their individual accession numbers, are listed. The septin proteins, KIAA0128, CDC10, NEDD5, and H5, are named after their human or mouse counterparts.

septins are also localized to the cleavage furrow of dividing mammalian cells (Figure 3A). In cultured, postmitotic hippocampal neurons, CDC10 shows a punctate distribution throughout the neurons (Figure 3B). A similar punctate CDC10 staining pattern was observed in neuroendocrine PC12 cells, although the CDC10 puncta were enriched near the plasma membrane, suggesting that a large population of septins are localized near the plasma membrane (data not shown). Costaining of hippocampal neurons in cultures with antibodies against synaptophysin, a synaptic vesicle marker, and CDC10 (Figures 3B, 3C, and 3D) demonstrated that the majority of CDC10 is not present in mature presynaptic nerve terminals.

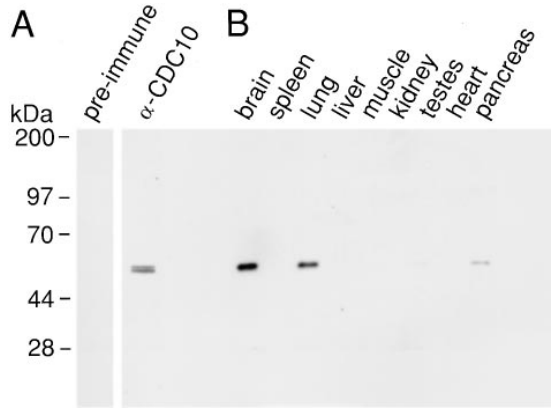

Figure 2. Tissue Distribution of CDC10 Septin

(A) Western blot detection of CDC10 immunoreactive proteins in brain homogenate.

(B) Regional Western blot analysis of CDC10 immunoreactive proteins. Twenty-five micrograms of postnuclear supernatants from the indicated rat tissues were loaded per lane.

Purification of the sec6/8 and Septin Complexes

To purify the septin and sec6/8 complexes for further characterization, soluble rat brain proteins were fractionated by four sequential chromatographic steps: hydroxyapatite, TMAE anion exchange, HW55-S gel filtration, and a second TMAE anion exchange column chromatography. The enrichment of the septin and sec6/8 complexes following each chromatographic step was monitored by Western blotting using antibodies against rat CDC10, sec6, and sec8, or by Coomassie blue staining (Figure 4). Interestingly, the purification of the septin complex partially overlapped with that of the sec6/8 complex. Both complexes bound to the hydroxyapatite matrix and coeluted in response to increasing phosphate concentration (Figure 4A). When the pooled

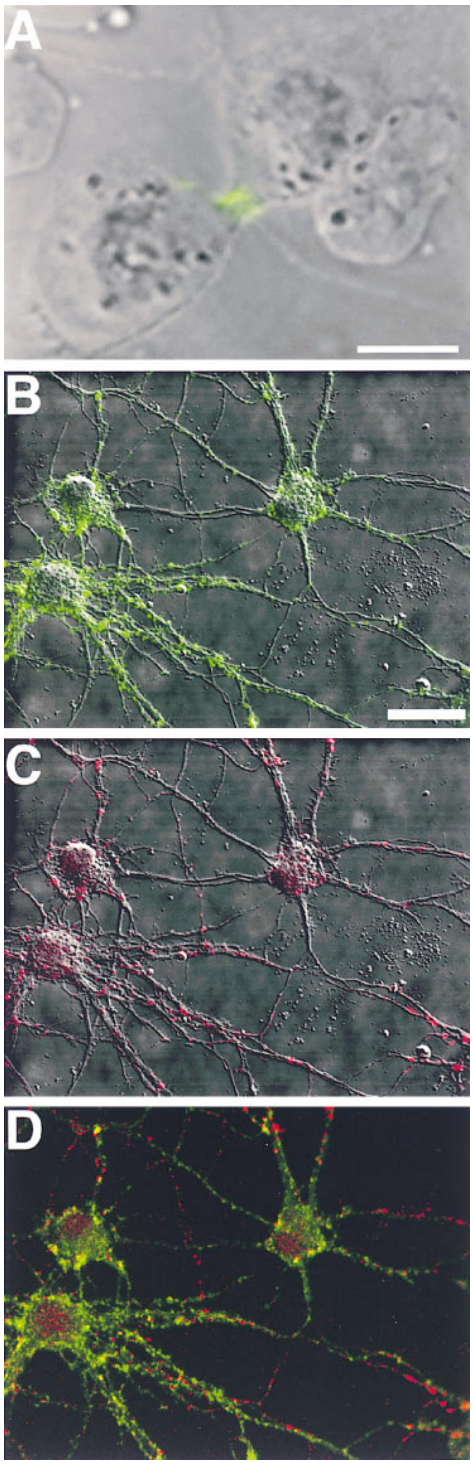

Figure 3. Localization of Septins in Dividing Cells and Cultured Hippocampal Neurons

Mammalian septins are present in both dividing and nondividing cells.

(A) CDC10 is found at sites of cytokinesis in dividing MDCK cells. Scale bar, 5.4 μm.

(B) Septin distribution (green) in 18-day-old cultured embryonic hippocampal neurons. Scale bar for (B), (C), and (D), 18.8 μm.

(C) Synaptophysin labeling (red) of the same neurons shown in (B).

(D) Overlay of the septin and synaptophysin staining.

hydroxyapatite column eluant was applied to a TMAE anion exchange column, both complexes again bound to the resin. The elution of the septin complex further overlapped with that of the sec6/8 complex from the TMAE column, although the majority of the septin complex eluted earlier from the column (Figure 4B). In fact, at this stage of purification, the septins, but not the sec6/8 complex, could be visualized on a Coomassie blue–stained sodium dodecyl sulfate (SDS) -polyacrylamide gel, suggesting that the septins are present in much larger quantities (at least 10-fold more) than the sec6/8 complex (data not shown). The TMAE eluant fractions enriched in the sec6/8 complex that still contained CDC10 immunoreactivity were pooled and further fractionated on a HW55-S gel filtration column. Following this chromatographic step, the sec6/8 complex with its eight subunits ranging from 70–110 kDa could be visualized on a Coomassie Blue–stained SDS-polyacrylamide gel as previously shown (Figure 4C; Hsu et al., 1996). Western blot analysis revealed that the CDC10 immunoreactivity eluted in a single broad peak before the sec6/8 complex from the gel filtration column (data not shown). On a Coomassie blue–stained SDS-polyacrylamide gel, the elution of five proteins ranging from 44–52 kDa coincided exactly with the elution of the CDC10 immunoreactivity (data not shown). These five proteins constituted at least 90% of the total proteins in the peak CDC10 immunoreactive column fractions and have identical molecular weights to the five proteins that coimmunoprecipitated with the sec6/8 complex (Figures 4C and 1B). To investigate the identities of these proteins, peptide sequencing analyses were carried out as previously described (Hsu et al., 1996). Peptides from these five protein bands (Table 1 and Figure 7) confirmed that they are identical to the septins that coimmunoprecipitated with the sec6/8 complex. The copurification of these septin proteins suggests that they may be subunits of a single, large septin complex. Finally, the sec6/8 complex was purified over a second TMAE anion exchange column. The major contaminant in the sec6/8 complex preparation at this stage is the septin complex (Figure 4D). This purification pattern is consistent with an association between the sec6/8 and the septin complexes. These two large complexes may be dissociating from each other throughout the purification process, suggesting a moderate affinity between the two complexes.

To examine whether the sec6/8 and septin complexes interact specifically with each other, immunoprecipitation with anti-rat sec8 monoclonal antibody 2E12 was performed at various stages of the septin complex purification (Figures 5A and 5B). The immunoprecipitation results were analyzed both by Coomassie blue staining of SDS-polyacrylamide gels (Figure 5A) and by Western blotting (Figure 5B). The septin complex coimmunoprecipitated with the sec6/8 complex following hydroxyapatite (HT), TMAE anion exchange (TMAE), and HW55-S gel filtration (GF) chromatography. In fact, after the gel filtration column step, the sec6/8 complex coimmunoprecipitated with the septin proteins in the absence of other major protein bands, indicating that the two complexes may associate with each other directly, in the absence of other intermediary proteins. However, since the ratio of the septins coimmunoprecipitating with the

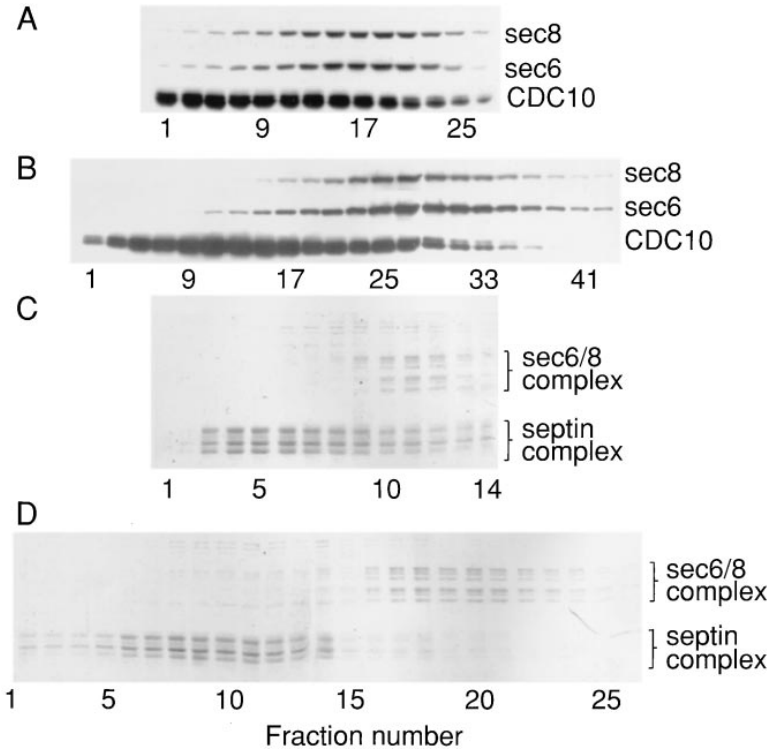

Figure 4. Purification of the sec6/8 and Septin Complexes

Both the sec6/8 and septin complexes were purified by fractionating soluble brain proteins over four sequential columns: hydroxyapatite (A), TMAE anion exchange (B), HW55-S gel filtration (C), and TMAE anion exchange (D). For the first two columns (the hydroxyapatite and the first TMAE anion exchange columns), the purification process was analyzed by Western blotting using anti-CDC10 polyclonal antibodies to monitor the elution of the septin complex and anti-rat sec6 and anti-rat sec8 monoclonal antibodies to monitor the elution of the sec6/8 complex. For the next two columns (the HW55-S gel filtration and the second TMAE anion exchange columns), the sec6/8 complex and the septin complexes were visualized by Coomassie blue staining of SDS-polyacrylamide gels.

sec6/8 complex decreases as the purification process progresses, other proteins may be involved in strengthening the interaction between these two complexes.

To further investigate this interaction, a reciprocal immunoprecipitation study using polyclonal antibodies against the septin protein, CDC10, was performed. First, anti-CDC10 antibodies immunoprecipitated all five septin bands, corresponding to four septins (KIAA0128, CDC10, NEDD5, and H5), suggesting that these four septins are subunits of a single septin complex. Second, after purification over the gel filtration column (GF), the sec6/8 complex coimmunoprecipitated with the septin complex in the absence of other proteins, further confirming an interaction between these two complexes (Figures 5A and 5B, GF column, α-CDC10 lane). As controls, isolated pure sec6/8 complex or septin complex was immunoprecipitated with the above antibodies. Anti-CDC10 polyclonal antibodies immunoprecipitated the purified septin complex but not the purified isolated sec6/8 complex (Figure 5C, septin column). Likewise, anti-rat sec8 monoclonal antibody 2E12 immunoprecipitated the sec6/8 complex but not the purified isolated septin complex (Figure 5C, sec6/8 complex row). These controls indicate that the coimmunoprecipitation of the sec6/8 complex with the septin complex was not due to the cross-reactivity of anti-rat sec8 or anti-rat CDC10 antibodies to both complexes.

The localization of the sec6/8 and septin complexes was examined in vivo by immunocytochemistry. In cultured hippocampal neurons, both complexes showed punctate distributions (Figures 6A and 6B). A partial overlap in their localization is consistent with an in vivo interaction between the sec6/8 and septin complexes (Figure 6C). If, however, the interaction between these complexes is dynamic and regulated, histochemical studies will not necessarily reveal either the full extent or the cellular sites of the interaction.

The purified sec6/8 complex contains eight subunits, which are approximately equally stained by Coomassie blue, suggesting a 1:1 stoichiometry among the subunits in the complex (Figure 7A). Seven of the eight subunits in the mammalian complex have been identified (Ting et al., 1995; Hsu et al., 1996; Guo et al., 1997; Hazuka et al., 1997; Kee et al., 1997), and the eighth subunit of 106 kDa is likely to be the mammalian homolog of the yeast sec3 protein (TerBush et al., 1996). The mammalian sec6/8 complex has a predicted molecular weight of 734 kDa, assuming one copy of each subunit per complex. This is consistent with the observed molecular weights of 600–650 kDa by glycerol gradient centrifugation analysis (Hsu et al., 1996) and 750 kDa by gel filtration chromatography on a Superose 6 HR column (Figure 7B). The mammalian sec6/8 complex appeared to be smaller than the globular thyroglobulin marker in glycerol gradient studies (Hsu et al., 1996) but exhibited a larger mass than thyroglobulin in gel filtration column chromatography (Figure 7B). This discrepancy suggests an extended and nonglobular conformation for the complex.

The purified septin complex was also characterized biochemically. On a Coomassie blue–stained SDS-polyacrylamide gel, it appears as five protein bands ranging in molecular weight from 44–52 kDa (Figure 7). Peptide sequence analyses of these protein bands identified them as the mammalian homologs of yeast and *Drosophila* septin proteins (Table 1, bands 1–5). Peptide sequences derived from the largest protein band at 52 kDa (KIAA0128) were identical in sequence to a human

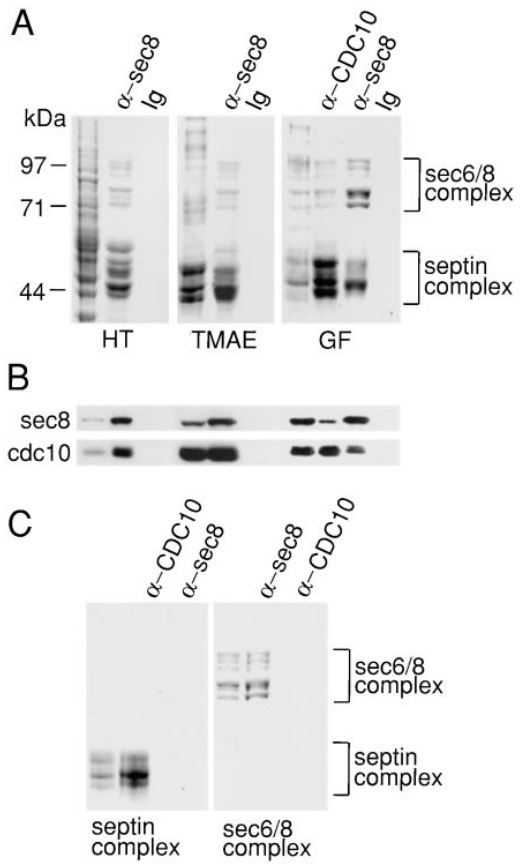

Figure 5. The sec6/8 Complex Interacts with a Septin Complex

The sec6/8 complex coimmunoprecipitates with the septin complex following hydroxyapatite (HT), TMAE anion exchange (TMAE), and HW55-S gel filtration (GF) column chromatography. The immunoprecipitation results were analyzed both by Coomassie blue staining of SDS-polyacrylamide gels (A) and by Western blotting (B), using anti-rat sec8 mouse monoclonal antibody to detect the sec6/8 complex and affinity-purified anti-CDC10 polyclonal antibodies to detect the septin complex. The first lane of each gel shows the pooled column fractions for immunoprecipitation. The column fractions were immunoprecipitated by either anti-rat sec8 monoclonal antibody 2E12 (α-sec8), affinity-purified anti-CDC10 polyclonal antibodies (α-CDC10), or nonspecific control immunoglobulins (Ig). The specificity of the anti-rat sec8 and anti-CDC10 antibodies was examined in (C). Purified septin and sec6/8 complexes were subjected to immunoprecipitation by anti-rat sec8 and anti-CDC10 antibodies. The first lane of each gel shows the purified complex used for immunoprecipitation.

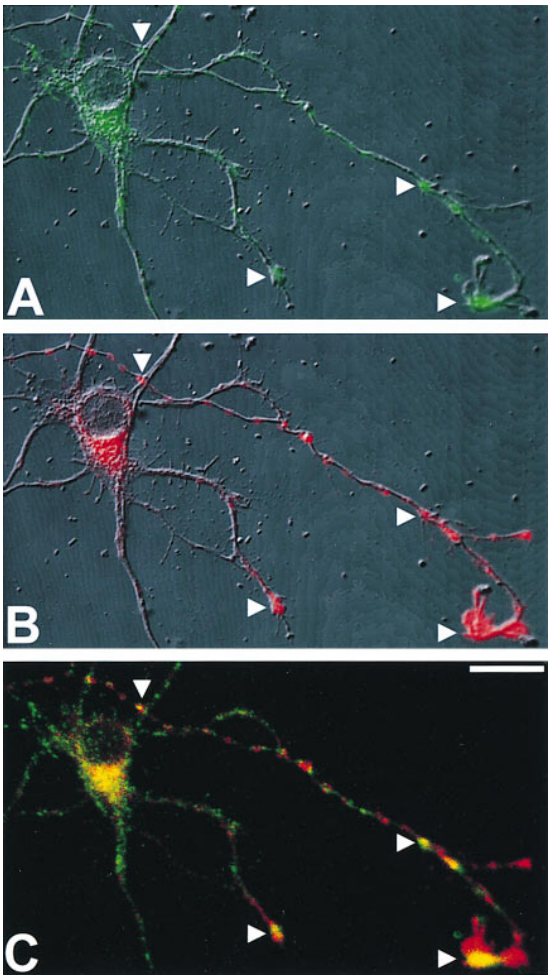

Figure 6. Localization of sec6/8 and Septin Complexes in Cultured Hippocampal Neurons

Sec6/8 and septin complexes display partial colocalization in hippocampal neurons.
(A) 6-day-old cultured embryonic hippocampal neurons labeled with antibodies against a septin protein CDC10 (green).
(B) The same neurons stained with monoclonal antibody 9H5 against sec6 (red), a subunit of the sec6/8 complex.
(C) Overlay of the sec6 and CDC10 staining. The arrows show overlaps in sec6 and CDC10 staining. Scale bar, 12 μm.

septin, KIAA0128 (Nagase et al., 1995). Peptides obtained from protein bands (CDC10) at 50 kDa and 48 kDa corresponded to the human homolog of the yeast septin protein CDC10 (hCDC10; Nakatsuru et al., 1994). These two bands may represent differentially modified CDC10 or degraded products of CDC10. Three peptides from the 50 kDa protein band matched to KIAA0128, probably due to the comigration of a degraded product of KIAA0128 with CDC10 on the SDS-polyacrylamide gel. The protein band of 46 kDa (NEDD5 and H5) yielded peptides identical in sequence to two mammalian septins, human DIFF6/mouse NEDD5/KIAA0158 (Nagase et al., 1995) and human H5/human CDCrel-1/human PNUTL1 (Zieger et al., 1997). The smallest septin band, at 44 kDa, is found to be H5. It is possible that H5 exists in two differentially modified forms. Alternatively, the band at 44 kDa may be a degradation product of H5.

Quick-Freeze/Deep-Etch Electron Microscopic Analysis of the sec6/8 and Septin Complexes

To visualize the structure of the sec6/8 complex, purified samples were adsorbed onto mica chips either with or without fixation with 40 mM glutaraldehyde (Figure 9). The mica chips were then quickly frozen, deep-etched, and rotary shadowed with platinum as previously described (Heuser, 1983, 1989). In the absence of glutaraldehyde fixation, the complex displays a variety of extended forms, presumably representing various distortions that occurred during adsorption to mica (Figure 9, top row).

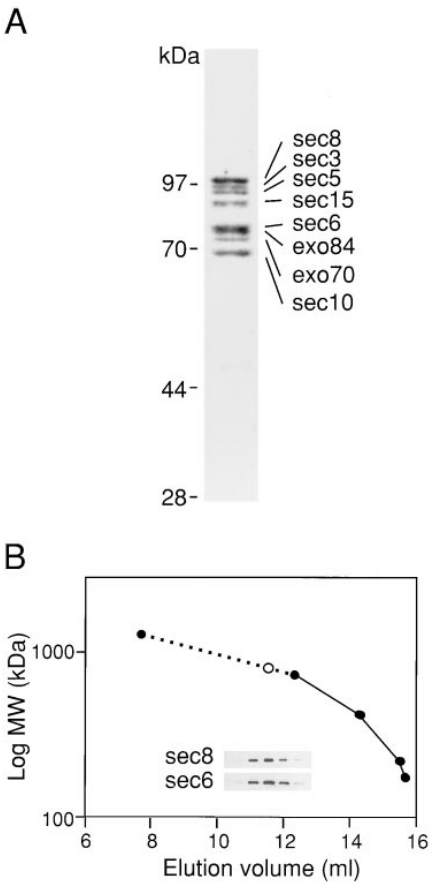

Figure 7. Subunit Composition and Gel Filtration Analysis of the sec6/8 Complex

(A) Coomassie blue–stained SDS-PAGE analysis of the purified sec6/8 complex used for electron microscopic studies.

(B) Gel filtration behavior of the purified sec6/8 complex on a Superose 6 HR column. The gel filtration column was calibrated against four molecular weight standards (closed circles from right to left): aldolase (177 kDa), catalase (200 kDa), ferritin (421 kDa), and thyroglobulin (733 kDa). The standard errors of calibration were $<0.5\%$. The elution of Blue dextran (2000 kDa) marks the void volume of the column (closed circle on the left). The elution of the sec6/8 complex from the column (open circle) was detected by Western blotting using anti-rat sec6 and anti-rat sec8 monoclonal antibodies (inset). The molecular weight of the sec6/8 complex was extrapolated from a calibration curve constructed from the elution patterns of the four molecular weight markers (solid line) and of Blue dextran (dotted line).

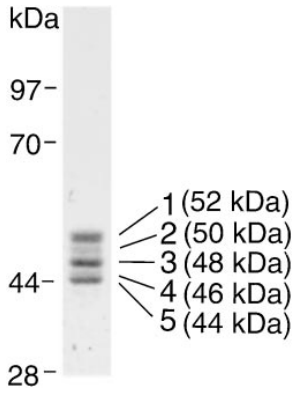

Figure 8. The Purified Mammalian Brain Septin Complex

Coomassie blue–stained SDS-PAGE analysis of the purified septin complex used for electron microscopic studies.

Generally, it appears as a set of four to six "arms" that radiate from a central point. These arms range from 4–6 nm in width and 10–30 nm in length and often appear to be split internally along their lengths. Prefixation with 40 mM glutaraldehyde for 5 min before adsorption to mica yields a more compact structure for the sec6/8 complex (Figure 9, second row and first four images of third row). In agreement with its hydrodynamic properties (Figure 6B), it appears to have a slightly elongated "body" of roughly the size and shape of thyroglobulin (Figure 9, thyroglobulin in last two images of third row), plus two arms that splay from one end of the body. Again, these arms are ~15 nm long and 6 nm wide, suggesting that they represent a subset of the shorter arms seen in unfixed complexes. Presumably, the longer arms pack together to form the body of the fixed samples. The body measures 30 nm long and 13 nm wide and is slightly tapered. The two arms appear to attach to the body through a flexible region since they extend away from the body at varying angles.

Visualization of the purified mammalian brain septin complex by deep-etch electron microscopy revealed ~8 nm wide filaments of variable lengths (Figure 9, bottom row). These appear similar to previously published images of yeast and *Drosophila* septin filaments (Byers and Goetsch, 1976; Haarer and Pringle, 1987; Ford and Pringle, 1991; Kim et al., 1991; Field et al., 1996). An interesting pattern emerges when the lengths of the mammalian septins are quantified. The most common mammalian septin lengths are 25 nm and 2×25 nm, or 50 nm (Figure 9, bottom row). This is strikingly similar to the lengths of the shortest septin filaments isolated from *Drosophila* (Field et al., 1996), but in that case, much longer filaments are also observed. Occasionally, longer septin filaments are also seen in the mammalian preparations, but their paucity suggests that longer ones, if they exist in mammals, must have been severed or dissociated during the purification process used here. In spite of these length preferences, the mammalian septin filaments, like their invertebrate counterparts, are likely to be constructed by repeated end-to-end annealing of "unit" lengths. We could discern no helical repeat or other periodicity along the length of the longer filaments. The mammalian septins are distinguishable from yeast and *Drosophila* septin filaments only in that they frequently display very thin strands emanating from their sides (Figure 9, bottom row; strands can be seen below each filament). These strands measure ~10–12 nm in length and tend to occur in relatively regular ~16 nm repeats. It is not obvious from the images whether these are partially denatured septin subunits or filament-associated proteins present at low levels in the mammalian preparations. Further studies will be required to better understand the structural underpinnings and functional significance of the septin "unit-element" organization observed here.

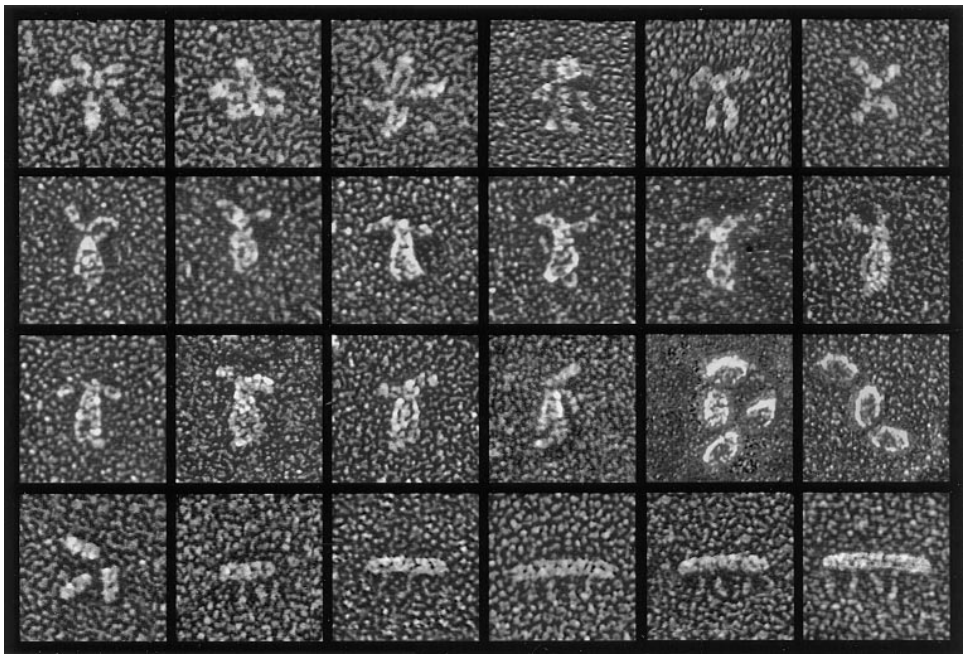

Figure 9. Structure of the Mammalian Brain sec6/8 and Septin Complexes

The top row shows the structure of purified sec6/8 complex when adsorbed to mica in the unfixed state. The complex adopts a series of radially symmetric conformations composed of "arms" of different lengths. The center rows show the structure of purified sec6/8 complex when adsorbed to mica after fixation in 40 mM glutaraldehyde for 5 min. Prefixation yields a more regular structure in which a relatively fat "body" is capped by just two arms, each similar in length to the shorter arms seen in unfixed complexes. The last two images of the third row show, for comparison, the structure of thyroglobulin, the molecular weight standard that most closely matches the rsec6/8 complex. The bottom row shows the structure of the mammalian septin complex. After adsorption to mica, the complex appears as a short ~8 nm filament with a "unit" length of 25 nm or 2 × 25 nm (see text). Mammalian septin filaments also commonly display thin strands projecting outward from their lateral edges. Magnification, 243,000×.

Discussion

Numerous filament proteins, including tubulin, actin and neurofilaments, play critical roles in establishing and maintaining neuronal morphology and membrane trafficking patterns. A fourth family of filaments, the septins, are considerably less well understood, in terms of both their structures and their functions in postmitotic cells. Here, we determined amino acid sequences corresponding to four septin proteins isolated from rat brain. The subunits of the rat brain septin filaments show a high degree of sequence homology to each other (34%–75%) and are similar in molecular weight, ranging from 44–52 kDa. The comigration of these four proteins through several columns and their coimmunoprecipitation by antibodies against one of the septins, CDC10, indicate that they are likely components of the same complex. The broad septin elution peak resulting from gel filtration chromatography is consistent with filaments of variable length, likely owing to severing into fragments of varying lengths during the homogenization or purification process. Using freeze-fracture, deep-etch electron microscopy, we demonstrated that the septin complex, similar to previously published yeast and *Drosophila* counterparts, forms filaments of ~8 nm in diameter. The length preferences exhibited in unit repeats of 25 nm are likely to be inherent properties of the ways in which the septin subunits assemble.

Like other members of the family, the mammalian brain septins all contain conserved GTPase motifs (reviewed by Longtine et al., 1996; G1, GXXXXGK(S/T); G3, DXXG; and G4, XKXD). Both GTP binding and GTPase activities have been demonstrated in *Drosophila* and mammalian septins. Immunoaffinity-purified *Drosophila* septin filaments composed of Sep1, Sep2, and PNUT exhibited GTP binding and GTPase activities, although these activities did not affect the polymerization state of the septin filament in vitro (Field et al., 1996). However, both microinjection of GTPγS and transfection of GTP-binding mutants of mouse NEDD5 septin into HeLa cells disrupted NEDD5-containing filaments, suggesting that the GTPase activity is required for mammalian septin filament formation in vivo (Kinoshita et al., 1997). Further studies will determine the functional significance of the GTP binding and GTPase activity of the mammalian septins.

The yeast septin filament is composed of four proteins, cdc3p, cdc10p, cdc11p, and cdc12p (Byers and Goetsch, 1976; Haarer and Pringle, 1987; Ford and Pringle, 1991; Kim et al., 1991). The *Drosophila* septin filament contains three septins, PNUT, Sep2, and Sep3 (Field et al., 1996). Presently, six mammalian septins have been identified (KIAA0128, Nagase et al., 1995; hCDC10, Nakatsuru et al, 1994; NEDD5, Kumar et al., 1992; Kinoshita et al., 1997; human H5, Zieger et al., 1997; mouse H5, Kato, 1990; and Diff 6, Nottenburg et al., 1990), and the rat analogs of four of these six septins (KIAA0128, CDC10, NEDD5, and H5) are constituents

of the septin filament characterized in this report. The remaining two rat septins as well as other yet to be identified mammalian proteins may form additional septin complexes that interact with different target proteins. A heterogeneity in septin filament composition and septin interacting proteins may allow these filaments to participate in a wide variety of processes in different cell types, at various stages of the cell cycle, and during different periods of development.

Septins have a well studied role in cytokinesis; however, these proteins are also abundant in adult rat brain, where terminally differentiated nerve cells no longer undergo cell division. High levels of expression are also observed in differentiated neurons in culture. Additionally, the mouse NEDD5 septin has been found to be more abundant in human fibroblast and SiHa cells when they are growth-arrested by serum starvation or contact inhibition than when they are actively dividing (Kinoshita et al., 1997). What is the function of septin filaments in these nondividing cells? The septins have been implicated in a myriad of processes, which can be divided into two major classes. First, the septins are localized to the leading edge of membrane extensions—for example, during the prospore wall formation in sporulating yeast (Fares et al., 1996) and during the cellularization of the syncytial blastoderm into individual cells in developing *Drosophila* embryos (Neufeld and Rubin, 1994; Fares et al., 1995). Second, the septins are involved in the generation of cell polarity. In yeast, the septins have been found to play a role in the proper localization of proteins required for bud site selection (Flescher et al., 1993; Chant et al., 1995) and for pheromone-induced mating projection (Konopka et al., 1995). In *Drosophila*, Sep1 and PNUT septins are localized to specialized membrane domains in polarized cells (Neufeld and Rubin, 1994; Fares et al., 1995), although the precise localization of the septins varies with cell types. Nevertheless, despite their pleiotropic functions in cytokinesis and in the generation and/or maintenance of cell polarity, the septins appear to carry out a singular task: the recruitment of proteins and membranes to establish and/or maintain specialized domains on the plasma membrane, a likely task in neurons as well.

How might the septin filaments and the sec6/8 complex target secretory vesicles to specialized domains of the plasma membrane? Previously, we identified and isolated the mammalian sec6/8 complex, a homolog of the yeast sec6/8/15 complex, which is essential for secretion in yeast (Hsu et al., 1996). The sec6/8 complex is composed of eight novel mammalian proteins; its widespread tissue distribution indicates that it is a ubiquitous part of the exocytosis machinery. The sec6/8 complex has an elongated body with two arms projecting outward at varying angles from one end. The length of the sec6/8 complex body is ~30 nm. While no known nucleotide-binding motifs have yet been found in the sec6/8 complex subunits, the unique morphology and the large size of the sec6/8 complex suggest that it may act as a link connecting two or more ligands. Perhaps the sec6/8 complex has the capacity to bridge the cytoskeleton and secretory vesicles, resulting in the recruitment and targeting of secretory vesicles to distinct sites. Targeting of vesicles containing specific cargoes to appropriate sites of protein and membrane addition may rely on interactions between the septin filaments and the sec6/8 complex. It is possible that sites of interaction between septin filaments and the sec6/8 complex may serve as a focal point for recruiting and targeting multiple proteins and vesicles through subunit-specific interactions with different protein ligands.

The sec6/8 and septin complexes may play a role in establishing exocytic sites on neuronal membrane during development and outside of synaptic sites in mature organisms. Thus, in developing neurons, the sec6/8 and septin complexes may be involved in determining the initial polarity of neuronal processes and/or the early establishment of synapses. Once synapse formation is complete, the mature synaptic vesicles cycle near the active zones, where they undergo repeated docking and fusion cycles at predetermined exocytic sites and may not require targeting by the sec6/8 or the septin complex. In MDCK cells, however, the sec6/8 complex appears to be required for the establishment and continuing maintenance of exocytic sites for the docking and fusion of Golgi-derived vesicles. Likewise, the presence of the septin and sec6/8 complexes in mature neurons suggests that these complexes may be needed for the maintenance of neuronal polarity as well as for process outgrowth during remodeling of neuronal connections, a process important for synaptic plasticity.

To carry out their functions, both the sec6/8 complex and the septin filaments must be targeted to and bind to specific plasma membrane receptors. Once they are localized to the plasma membrane, they may either recruit additional proteins and/or become components of a "targeting patch" or a potential docking/fusion site for vesicles (reviewed by Drubin and Nelson, 1996). The composition of this targeting patch is still unknown although extraction of the membrane-bound sec6/8 complex using the detergent Triton X-100 revealed that approximately half of the sec6/8 complex is associated with a Triton X-100–insoluble receptor, possibly composed of cytoskeletal elements (Hsu et al., 1996). In this regard, it is of interest that a genetic interaction has been observed between yeast sec3 and profilin, an actin-associated protein (Finger and Novick, 1997). Likewise, mutations in yeast septins also affected actin filament organization during yeast budding (Adams and Pringle, 1984). In light of the results we have shown in this paper, the interaction of the sec6/8 complex with the septin filament may account, in part, for the Triton X-100 insolubility of the membrane-bound sec6/8 complex. It is interesting to note, however, that in yeast the sec6/8 complex can be recruited to the plasma membrane independent of septins. At the beginning of the yeast budding process, the sec6/8 complex is recruited to the tip of the growing daughter cell in the absence of septin accumulation at that site (TerBush and Novick, 1995; Mondésert et al., 1997). As cell division progresses, the sec6/8 complex and the septin filaments accumulate at the mother–daughter cell boundary prior to cytokinesis. Thus, it is likely that the sec6/8 and septin complexes can be recruited either independently or together to the plasma membrane, where they may function either by themselves or in a synergistic manner to recruit distinct protein and vesicle cargoes in response to different cellular

requirements. Furthermore, in mammalian MDCK cells, the sec6/8 complex does not associate with the plasma membrane until E-cadherin–mediated cell adhesion is established (K. Grindstaff, C. Yeaman, N. Anandasabapathy, S.-C. H., E. Rodriguez-Boulan, R. H. S., and W. J. Nelso, submitted). This suggests that the recruitment of the sec6/8 complex and perhaps the septin filaments is not only spatially but also temporally regulated. It remains to be seen how these two complexes are targeted to and anchored at various specialized domains of the plasma membrane in response to different biochemical cues at different stages of the cell cycle and development.

The identification and characterization of many potential protein players in the secretory pathway has provided us with a glimpse into the molecular events underlying exocytosis. Following the biogenesis of secretory vesicles, the vesicles must be vectorially transported to the vicinity of a targeting site, which we propose is comprised of the sec6/8 complex, and perhaps of other proteins, on the plasma membrane. Once vesicles are at the targeting patch, SNARE proteins function through the formation of a trimeric syntaxin/SNAP25/VAMP complex, which brings the vesicle and the plasma membrane close together to promote fusion of the lipid bilayers. Small GTPases, such as those of the rab protein family, have been implicated in playing an important role in the exocytic pathway, although the mechanisms of their action remain unclear (Pfeffer, 1994; Novick and Zerial, 1997). Genetic studies show that overexpression of a yeast low molecular weight GTPase, sec4, can suppress mutations in five subunits (sec3, sec5, sec8, sec10, and sec15) of the yeast sec6/8 complex, suggesting an interaction between the sec6/8 complex and the small GTP-binding proteins (Brennwald et al., 1994). Characterization of the interactions among the targeting patch, the connecting cytoskeleton/motor network, and other components of the exocytosis machinery will allow further insights into both the vesicle trafficking process and eventually the modulation of vesicle trafficking during learning and memory.

Experimental Procedures

Immunoprecipitation Studies

Anti-rat sec8 mouse monoclonal antibody 2E12 and affinity-purified anti-CDC10 rabbit polyclonal antibodies were coupled to protein G and protein A beads, respectively, at a final concentration of 2 mg/ml using the cross-linker dimethylpimelimidate as previously described (Pevsner et al., 1994). For controls, nonspecific rabbit and mouse immunoglobulins were also coupled to protein A and protein G beads, respectively. Soluble brain proteins and pooled column fractions were precleared with either protein A or protein G beads (10 μl protein G beads per 100 μl protein sample) at 4°C for 4 hr. The precleared protein samples were then incubated with immobilized anti-rat sec8, anti-rat CDC10, or control antibodies overnight at 4°C. The next day, the beads were washed two times with 10 vol 20 mM Tris (pH 8.0) and 0.15 M NaCl (buffer A) containing 1 mg/ml soybean trypsin inhibitor, two times with 10 vol buffer A, and finally two times with 10 vol buffer A containing 0.1% Tween 20. Proteins bound to the beads were solubilized in protein sample buffer containing 10% SDS and subjected to SDS-polyacrylamide gel electrophoresis (SDS-PAGE) and Western blot analyses.

Antibodies and Western Blot Analyses

Monoclonal antibodies against rat sec6 and rat sec8 were obtained from the corresponding mouse hybridoma cell lines generated by fusion of mouse NS-1 myeloma cells with spleen cells from Balb/c mice immunized with histidine-tagged rat sec6 and rat sec8 fusion proteins, respectively (Lane et al., 1986). Anti-rat sec6 monoclonal antibody 9H5 and anti-rat sec8 monoclonal antibody 14G1 were used for Western blot analyses. Both monoclonal antibodies detect a single band corresponding to their respective antigens in brain homogenate. Anti-CDC10 rabbit polyclonal antibodies were generated against a C-terminal peptide of hCDC10 (peptide sequence NH_2-RILEQQNSSRTLGKNKKKGKIF-COOH, corresponding to amino acids 397–418 of hCDC10) and affinity purified as previously described (Pevsner et al., 1994).

Tissue Distribution of CDC10 Septin

Rat tissue samples were prepared as previously described (Ting et al., 1995) and subjected to Western blot analysis.

Purification of the sec6/8 and Septin Complexes

The sec6/8 and septin complexes were both purified from frozen rat brains using four sequential chromatographic steps as previously described for the sec6/8 complex purification (Hsu et al., 1996). Fractions containing the purified sec6/8 and septin complexes were pooled and subjected to SDS-PAGE and electron microscopic analyses. Following fractionation by SDS-PAGE, individual bands of the purified septin complex were excised and subjected to in-gel proteolysis and peptide sequencing at the Stanford Pan facility.

Gel Filtration Behavior of the sec6/8 Complex

Two hundred microliters of molecular weight standard (containing 500 μg thyroglobulin, 10 μg ferritin, 500 μg catalase, and 500 μg aldolase) or purified sec6/8 complex was fractionated over a Superose 6 HR 10/30 column (Pharmacia; bed dimension, 10 × 300 mm; bed volume, 24 ml) equilibrated in 50 mM sodium phosphate and 0.15 M NaCl (pH 7.0) at a flow rate of 0.2 ml/min. Fractions (500 μl) were collected, precipitated by trichloroacetic acid, fractionated by SDS-PAGE, and analyzed by Western blotting using anti-rat sec6 and anti-rat sec8 monoclonal antibodies.

Cell Cultures and Fluorescence Microscopy

Embryonic hippocampal cell cultures were prepared from the hippocampi of 18- to 19-day-old fetal rats as previously described (Banker and Cowan, 1977; Fletcher et al., 1991). Hippocampal cells were plated at a density of ~5000 cells/cm^2 on poly-L-lysine–coated coverslips, which were then placed in cultures of previously prepared astroglia. Cultures at 6 or 18 days in vitro were submerged in 4% paraformaldehyde for 20 min, extracted in 100% methanol at −20°C for 6 min, dehydrated, and rehydrated in phosphate buffered saline (PBS) containing 0.1 M glycine. MDCK cells were maintained as previously described (Adams et al., 1996). After plating the MDCK cells at a subconfluent density for 6 hr, the cells were extracted in CSK buffer (50 mM NaCl, 300 mM sucrose, 10 mM PIPES [pH 6.8], 3 mM $MgCl_2$, and 0.5% Triton X-100) on ice for 5 min, fixed in 4% paraformaldehyde for 20 min, and washed in PBS containing 0.1 M glycine. Cell staining was carried out as previously described (Kee et al., 1997). Differential interference contrast (DIC), fluorescein, and Cy5 signals were obtained simultaneously using a scanning confocal microscope developed by Drs. Stephen J. Smith and Noam Ziv (Stanford University).

Electron Microscopic Imaging

Purified sec6/8 and septin complexes were adsorbed to mica flakes either with or without 5 min fixation in 40 mM glutaraldehyde and subjected to freeze-drying and platinum replication as previously described (Heuser, 1983, 1989). Thyroglobulin was purchased from Pharmacia as a lyophilized powder. Quantification of the lengths of the septin complexes was done by hand measurements of ~200 filaments.

Acknowledgments

We thank Jason Bock for computer assistance, Karen Peterson for assistance in hybridoma cell culture, Bing Yang for assistance in HPLC, Cindy Adams and Dr. Stephen J Smith for assistance with

confocal microscopy, and Alan Smith and Richard Winant at the Stanford Pan facility for peptide sequencing.

Received February 17, 1998; revised March 30, 1998.

References

Aalto, M.K., Ronne, H., and Keranen, S. (1993). Yeast syntaxins Sso1p and Sso2p belong to a family of related membrane proteins that function in vesicular transport. EMBO J. *12*, 4095–4104.

Adams, A.E.M., and Pringle, J.R. (1984). Relationship of actin and tubulin distribution to bud growth in wild-type and morphogenetic-mutant *Saccharomyces cerevisiae*. J. Cell Biol. *98*, 934–945.

Adams, C.L., Nelson, W.J., and Smith, S.J. (1996). Quantitative analysis of cadherin–catenin–actin reorganization during development of cell–cell adhesion. J. Cell Biol. *135*, 1899–1911.

Banker, G.A., and Cowan, W.M. (1977). Rat hippocampal neurons in dispersed cell culture. Brain Res. *126*, 397–342.

Brennwald, P., Kearns, B., Champion, K., Keranen, S., Bankaitis, V., and Novick, P. (1994). Sec9 is a SNAP-25–like component of a yeast SNARE complex that may be the effector of Sec4 function in exocytosis. Cell *79*, 245–258.

Broadie, K., Prokop, A., Bellen, H.J., O'Kane, C.J., Schulze, K.L., and Sweeney, S.T. (1995). Syntaxin and synaptobrevin function downstream of vesicle docking in Drosophila. Neuron *15*, 663–673.

Byers, B., and Goetsch, L. (1976). A highly ordered ring of membrane-associated filaments in budding yeast. J. Cell Biol. *69*, 717–721.

Catsicas, S., Catsicas, M., Keyser, K.T., Karten, H.J., Wilson, M.C., and Milner, R.J. (1992). Differential expression of the presynaptic protein SNAP-25 in mammalian retina. J. Neurosci. Res. *33*, 1–9.

Chant, J., Mischke, M., Mitchell, E., Herskowitz, I., and Pringle, J.R. (1995). Role of Bud3p in producing the axial budding pattern of yeast. J. Cell Biol. *129*, 767–778.

Drubin, D.G., and Nelson, W.J. (1996). Origins of cell polarity. Cell *84*, 335–344.

Fares, H., Goetsch, L., and Pringle, J.R. (1996). Identification of a developmentally regulated septin and involvement of the septins in spore formation in *Saccharomyces cerevisiae*. J. Cell Biol. *132*, 399–411.

Fares, H., Peifer, M., and Pringle, J.R. (1995). Localization and possible functions of *Drosophila* septins. Mol. Biol. Cell *6*, 1843–1859.

Field, C.M., al-Awar, O., Rosenblatt, J., Wong, M.L., Alberts, B., and Mitchison, T.J. (1996). A purified *Drosophila* septin complex forms filaments and exhibits GTPase activity. J. Cell Biol. *133*, 605–616.

Finger, F.P., and Novick, P. (1997). Sec3p is involved in secretion and morphogenesis in *Saccharomyces cerevisiae*. Mol. Biol. Cell *8*, 647–662.

Flescher, E.G., Madden, K., and Snyder, M. (1993). Components required for cytokinesis are important for bud site selection in yeast. J. Cell Biol. *122*, 373–386.

Fletcher, T.L., Cameron, P., De Camilli, P., and Banker, G. (1991). The distribution of synapsin I and synaptophysin in hippocampal neurons developing in culture. J. Neurosci. *11*, 1617–1626.

Ford, S.K., and Pringle, J.R. (1991). Cellular morphogenesis in the *Saccharomyces cerevisiae* cell cycle: localization of the CDC11 gene product and the timing of events at the budding site. Dev. Genet. *12*, 281–292.

Friedrich, G.A., Hildebrand, J.D., and Soriano, P. (1997). The secretory protein Sec8 is required for paraxial mesoderm formation in the mouse. Dev. Biol. *192*, 364–374.

Garcia, E.P., McPherson, P.S., Chilcote, T.J., Takei, K., and De Camilli, P. (1995). rbSec1A and B colocalize with syntaxin 1 and SNAP-25 throughout the axon, but are not in a stable complex with syntaxin. J. Cell Biol. *129*, 105–120.

Guo, W., Roth, D., Gatti, E., De Camilli, P., and Novick, P. (1997). Identification and characterization of homologs of the Exocyst component Sec10p. FEBS Lett. *404*, 135–139.

Haarer, B.K., and Pringle, J.R. (1987). Immunofluorescence localization of the *Saccharomyces cerevisiae* CDC12 gene product to the vicinity of the 10-nm filaments in the mother-bud neck. Mol. Cell Biol. *7*, 3678–3687.

Hanson, P.I., Roth, R., Morisaki, H., Jahn, R., and Heuser, J.E. (1997). Structure and conformational changes in NSF and its membrane receptor complexes visualized by quick-freeze/deep-etch electron microscopy. Cell *90*, 523–535.

Hay, J.C., and Scheller, R.H. (1997). SNAREs and NSF in targeted membrane fusion. Curr. Opin. Cell Biol. *9*, 505–512.

Hazuka, C.D., Hsu, S.-C., and Scheller, R.H. (1997). Characterization of a cDNA encoding a subunit of the rat brain rsec6/8 complex. Gene *187*, 67–73.

Heuser, J.E. (1983). Procedure for freeze-drying molecules adsorbed to mica flakes. J. Mol. Biol. *169*, 155–195.

Heuser, J. (1989). Protocol for 3-D visualization of molecules on mica via the quick-freeze, deep-etch technique. J. Electron Microsc. Tech. *13*, 244–263.

Hsu, S.-C., Ting, A.E., Hazuka, C.D., Davanger, S., Kenny, J.W., Kee, Y., and Scheller, R.H. (1996). The mammalian brain rsec6/8 complex. Neuron *17*, 1209–1219.

Hunt, J.M., Bommert, K., Charlton, M.P., Kistner, A., Habermann, E., Augustine, G.J., and Betz, H. (1994). A postdocking role for synaptobrevin in synaptic vesicle fusion. Neuron *12*, 1269–1279.

Kato, K. (1990). A collection of cDNA clones with specific expression patterns in mouse brain. Eur. J. Neurosci. *2*, 704–711.

Kee, Y., Yoo, J.S., Hazuka, C.D., Peterson, K.E., Hsu, S.C., and Scheller, R.H. (1997). Subunit structure of the mammalian exocyst complex [In Process Citation]. Proc. Natl. Acad. Sci. USA *94*, 14438–14443.

Kim, H.B., Haarer, B.K., and Pringle, J.R. (1991). Cellular morphogenesis in the *Saccharomyces cerevisiae* cell cycle: localization of the CDC3 gene product and the timing of events at the budding site. J. Cell Biol. *112*, 535–544.

Kinoshita, M., Kumar, S., Mizoguchi, A., Ide, C., Kinoshita, A., Haraguchi, T., Hiraoka, Y., and Noda, M. (1997). Nedd5, a mammalian septin, is a novel cytoskeletal component interacting with actin-based structures. Genes Dev. *11*, 1535–1547.

Koh, S., Yamamoto, A., Inoue, A., Inoue, Y., Akagawa, K., Kawamura, Y., Kawamoto, K., and Tashiro, Y. (1993). Immunoelectron microscopic localization of the HPC-1 antigen in rat cerebellum. J. Neurocytol. *22*, 995–1005.

Konopka, J.B., DeMattei, C., and Davis, C. (1995). AFR1 promotes polarized apical morphogenesis in *Saccharomyces cerevisiae*. Mol. Cell. Biol. *15*, 723–730.

Kumar, S., Tomooka, Y., and Noda, M. (1992). Identification of a set of genes with developmentally down-regulated expression in the mouse brain. Biochem. Biophys. Res. Commun. *185*, 1155–1161.

Lane, R.D., Crissman, R.S., and Ginn, S. (1986). High efficiency fusion procedure for producing monoclonal antibodies against weak immunogens. Methods Enzymol. *121*, 183–192.

Lin, R.C., and Scheller, R.H. (1997). Structural organization of the synaptic exocytosis core complex. Neuron *19*, 1087–1094.

Longtine, M.S., DeMarini, D.J., Valencik, M.L., Al-Awar, O.S., Fares, H., De Virgilio, C., and Pringle, J.R. (1996). The septins: roles in cytokinesis and other processes. Curr. Opin. Cell Biol. *8*, 106–119.

Mondésert, G., Clarke, D.J., and Reed, S.I. (1997). Identification of genes controlling growth polarity in the budding yeast *Saccharomyces cerevisiae*: a possible role of N-glycosylation and involvement of the exocyst complex. Genetics *147*, 421–434.

Nagase, T., Seki, N., Tanaka, A., Ishikawa, K., and Nomura, N. (1995). Prediction of the coding sequences of unidentified human genes. IV. The coding sequences of 40 new genes (KIAA0121–KIAA0160) deduced by analysis of cDNA clones from human cell line KG-1. DNA Res. *2*, 167–174.

Nakatsuru, S., Sudo, K., and Nakamura, Y. (1994). Molecular cloning of a novel human cDNA homologous to CDC10 in *Saccharomyces cerevisiae*. Biochem. Biophys. Res. Commun. *202*, 82–87.

Neufeld, T.P., and Rubin, G.M. (1994). The Drosophila *peanut* gene

is required for cytokinesis and encodes a protein similar to yeast putative bud neck filament proteins. Cell *77*, 371–379.

Nottenburg, C., Gallatin, W.M., and St. John, T. (1990). Lymphocyte HEV adhesion variants differ in the expression of multiple gene sequences. Gene *95*, 279–284.

Novick, P., and Zerial, M. (1997). The diversity of Rab proteins in vesicle transport. Curr. Opin. Cell. Biol. *9*, 496–504.

Novick, P., Field, C., and Schekman, R. (1980). Identification of 23 complementation groups required for posttranslational events in the yeast secretory pathway. Cell *21*, 205–215.

Oyler, G.A., Polli, J.W., Higgins, G.A., Wilson, M.C., and Billingsley, M.L. (1992). Distribution and expression of SNAP-25 immunoreactivity in rat brain, rat PC-12 cells and human SMS-KCNR neuroblastoma cells. Brain Res. Dev. Brain Res. *65*, 133–146.

Pevsner, J., Hsu, S.C., Braun, J.E., Calakos, N., Ting, A.E., Bennett, M.K., and Scheller, R.H. (1994). Specificity and regulation of a synaptic vesicle docking complex. Neuron *13*, 353–361.

Pfeffer, S.R. (1994). Rab GTPases: master regulators of membrane trafficking. Curr. Opin. Cell Biol. *6*, 522–526.

Rothman, J.E., and Wieland, F.T. (1996). Protein sorting by transport vesicles. Science *272*, 227–234.

Sanders, S.L., and Field, C.M. (1994). Cell division. Septins in common? Curr. Biol. *4*, 907–910.

Scheller, R.H. (1995). Membrane trafficking in the presynaptic nerve terminal. Neuron *14*, 893–897.

Südhof, T.C. (1995). The synaptic vesicle cycle: a cascade of protein–protein interactions. Nature *375*, 645–653.

TerBush, D.R., and Novick, P. (1995). Sec6, Sec8, and Sec15 are components of a multisubunit complex which localizes to small bud tips in *Saccharomyces cerevisiae*. J. Cell Biol. *130*, 299–312.

TerBush, D.R., Maurice, T., Roth, D., and Novick, P. (1996). The Exocyst is a multiprotein complex required for exocytosis in *Saccharomyces cerevisiae*. EMBO J. *15*, 6483–6494.

Ting, A.E., Hazuka, C.D., Hsu, S.C., Kirk, M.D., Bean, A.J., and Scheller, R.H. (1995). rSec6 and rSec8, mammalian homologs of yeast proteins essential for secretion. Proc. Natl. Acad. Sci. USA *92*, 9613–9617.

Zieger, B., Hashimoto, Y., and Ware, J. (1997). Alternative expression of platelet glycoprotein Ib(β) mRNA from an adjacent 5′ gene with an imperfect polyadenylation signal sequence. J. Clin. Invest. *99*, 520–525.

Note Added in Proof

The data referred to throughout as K. Grindstaff et al., submitted, have now been published: Grindstaff, K., Yeaman, C., Anadasabapathy, N., Hsu, S.-C., Rodriguez-Boulan, E., Scheller, R.H., and Nelson, W.J. (1998). Sec6/8 complex is recruited to cell–cell contacts and specifies transport vesicle delivery to the basal-lateral membrane in epithelial cells. Cell *93*, 731–740.